C.T. Ng

On accuracy of analytical modeling of Lamb wave scattering at delaminations in multilayered isotropic plates

http://hdl.handle.net/2440/94972

World Scientific
www.worldscientific.com

ON ACCURACY OF ANALYTICAL MODELING OF LAMB WAVE SCATTERING AT DELAMINATIONS IN MULTILAYERED ISOTROPIC PLATES

C.T. Ng

School of Civil, Environmental & Mining Engineering, The University of Adelaide,
Adelaide, SA 5005, Australia
alex.ng@adelaide.edu.au

The study investigates the accuracy of analytical solutions to the fundamental anti-symmetric Lamb wave scattering at delamination in multilayered isotropic plates. The analytical models are based on the wave function expansion method and Born approximation within the framework of Mindlin plate theory. The study validates the accuracy of modeling the delamination as an inhomogeneity with reduced bending rigidity in predicting Lamb wave scattering induced by geometry change at the delaminated region. A good agreement is observed between the analytical solutions and results of experimentally verified three-dimensional explicit finite element simulations. The findings support the inhomogeneity assumption in Lamb wave scattering problems and show the feasibility of employing it in delamination characterization.

Keywords: Lamb wave; scattering; delamination; Mindlin plate; wave function expansion; Born approximation; finite element; diffraction tomography.

1. Introduction

The use of Lamb waves in non-destructive evaluation (NDE) has attracted considerable attention in the last decade[1-4]. A variety of research has been conducted in an effort to improve the understanding of Lamb wave propagation and scattering at defects[5-12], and to develop innovative techniques for safety inspection of layered materials, such as adhesive and diffusion bonded isotropic plates[13-15] and composite laminates[16,17]. Among the developed damage inspection techniques, Lamb wave diffraction tomography (LWDT)[18,19] is proving attractive as it is not only able to determine the existence and location of defects, but can also provide quantitative information from the damage inspection, such as defect sizes and shapes. Recently a generic diffraction tomography framework was proposed for imaging damage in plates[20]. Numerical simulation and experimental data were used to demonstration the capability of the method.

The further development of the LWDT not only requires a scattering model that can reasonably predict the Lamb wave scattering but also an understanding of Lamb wave propagation and scattering characteristics at defects, especially for delaminations in thin layered structures. Recently a number of published papers have reported on the use of Lamb wave in layered materials, such as thin layered isotropic plates[13-15] and composite

laminates[16,17]. These layered materials have been widely employed in different engineering fields, such as aerospace, civil engineering, wind energy generation as well as land and water transport infrastructure. Lowe and Cawley[15] examined the Lamb wave propagation phenomenon in adhesive and diffusion bonded isotropic plates through dispersion curves. Two models, a perfect bonded structure without an adhesive layer and a bonded structure with a thin adhesive layer, were compared in the study. It showed that the fundamental symmetric (S_0) Lamb wave has increasing sensitivity to the presence of an adhesive layer in the bonded structures. In contrast, the fundamental anti-symmetric (A_0) Lamb wave is not sensitive to the presence of the adhesive layer as A_0 Lamb wave is characterized by bending of the plate, especially at low frequency. For composite materials, it has been discovered that the scattering characteristics of A_0 Lamb waves at defects in quasi-isotropic composite laminates are quite different from those scattering at defects in isotropic plates[21].

Researchers have observed that the stacking sequence of composite laminates greatly influences the scattering characteristics. It has been demonstrated that the Lamb wave scattering directivity pattern at the defects is dominated by the fiber orientation of the outer layers of the laminate, and are quite different for composite laminates that have the same number of laminae but with different stacking sequences. A recent study[22] investigated the results of modeling the delamination in composite laminates as an inhomogeneity based on the Mindlin plate theory with equivalent isotropic elastic properties assumption. It showed that the Lamb wave scattering at the delaminations is not well predicted by the analytical solutions, especially the backward scattering amplitudes, due to the stacking sequence influence of composite laminates. Hence, the fundamental assumption that the inhomogeneity with reduced bending rigidity could be used to represent the delaminated region in Lamb wave scattering problems has not been fully validated.

The current study therefore fills a gap by investigating the accuracy of modeling the delamination as the inhomogeneity in thin layered isotropic plates, allowing the stacking sequence influence to be ignored. Hence, the study evaluates the accuracy of using the inhomogeneity to model the scattered A_0 Lamb waves as an effect only due to the geometry change at the delaminated region, in which the plate divided into two individual sub-waveguides. In addition, the current study demonstrates the potential of using analytical solutions to predict Lamb wave scattering at delaminations in layered metallic structures[13-15] and suggests difficulties needed to be overcome for extending the LWDT, which has been developed based on the Born approximation within the framework of Mindlin plate theory, to delamination characterization. A three-dimensional (3D) explicit finite element (FE) model, which has been verified through a comprehensive experimental study[10], is used as a benchmark to assess the accuracy of predicting the A_0 Lamb wave scattering at delaminated regions using wave function expansion (WFE) method and Born approximation within the framework of Mindlin plate theory.

2. Analytical Solution for Wave Scattering from Inhomogeneity

2.1. *Wave function expansion method*

Within the framework of Mindlin plate theory, the scattering of A_0 Lamb waves by a cylindrical flexural inhomogeneity with radius a can be obtained using the WFE method[5] and Born approximation[23]. It is assumed that the thin adhesive layer can be ignored for the A_0 Lamb wave problems given the fact that it is not sensitive to the presence of the thin adhesive layer, especially at low frequency regime[15]. In polar coordinates the deflection potential of an incident wave at frequency W can be expressed as[22]

$$W^{(i)}(r,q) = \sum_{n=0}^{\infty} \hat{I}_n i^n J_n(k_1 r) \cos(nq) \tag{1}$$

where r and q are the radial and azimuthal coordinates of the polar coordination system. $i = \sqrt{-1}$ is the imaginary unit. The superscript (i) represents the parameters pertaining to the incident wave. $J_n(\times)$ is the n-th order Bessel function of the first kind, and $\hat{I}_0 = 1$ and $\hat{I}_n = 2$ for $n \geq 1$. Using the WFE method[5], the deflection (W) and rotation potentials (y_r, y_q) of the scattered wave at outside $(r > a)$ and inside $(r \leq a)$ the cylindrical inhomogeneity can be calculated by

$$W^{(s)} = \sum_{n=0}^{\infty} \left[A_{1n} H_n(k_1 r) + A_{2n} H_n(k_2 r) \right] \cos nq \tag{2}$$

$$y_r^{(s)} = \sum_{n=0}^{\infty} \left[I_1 A_{1n} k_1 H_n'(k_1 r) + I_2 A_{2n} k_2 H_n'(k_2 r) + A_{3n} \frac{n}{r} H_n(k_3 r) \right] \cos nq \tag{3}$$

$$y_q^{(s)} = -\sum_{n=0}^{\infty} \left[I_1 A_{1n} \frac{n}{r} H_n(k_1 r) + I_2 A_{2n} \frac{n}{r} H_n(k_2 r) + A_{3n} k_3 H_n'(k_3 r) \right] \sin nq \tag{4}$$

and

$$W^* = \sum_{n=0}^{\infty} \left[A_{1n}^* J_n(k_1^* r) + A_{2n}^* J_n(k_2^* r) \right] \cos nq \tag{5}$$

$$y_r^* = \sum_{n=0}^{\infty} \left[I_1^* A_{1n}^* k_1^* J_n'(k_1^* r) + I_2^* A_{2n}^* k_2^* J_n'(k_2^* r) + A_{3n}^* \frac{n}{r} J_n(k_3^* r) \right] \cos nq \tag{6}$$

$$y_q^* = -\sum_{n=0}^{\infty} \left[I_1^* A_{1n}^* \frac{n}{r} J_n(k_1^* r) + I_2^* A_{2n}^* \frac{n}{r} J_n(k_2^* r) + A_{3n}^* k_3^* J_n'(k_3^* r) \right] \sin nq \tag{7}$$

where $I_j = -1 + (12 W^2 r / p^2 G) k_j^{-2}$ for $j = 1, 2$. The superscript (s) and asterisk indicate

the variables related to the waves scattered from and transmitted into the cylindrical inhomogeneity, respectively. $H(\times)$ represents the n-th order Hankel function of the first kind. k_1, k_2 and k_3 are the wavenumbers below the first cut-off frequency and they can be calculated as[5]

$$k_j^2 = \frac{rw^2}{2}\left[\frac{1}{k^2 G} + \frac{(1-n^2)}{E}\right] \pm \sqrt{\frac{rw^2}{2} + \frac{rw^2}{4}\left[\frac{1}{k^2 G} + \frac{(1-n^2)}{E}\right]^2}, \quad j = 1,2 \qquad (8)$$

$$k_3^2 = k^2 \frac{k^2 k_1^2 k_2^2 E}{rw^2(1-n^2)} \qquad (9)$$

where $k = p/\sqrt{12}$. E, G, n and r are the Young's modulus, shear modulus, Poisson's ratio, and density of the plate, respectively. The unknown expansion coefficients A_{1n}, A_{2n}, A_{3n}, A_{1n}^*, A_{2n}^* and A_{3n}^* can be determined by substituting Eqs. (2) – (7) into the following continuity and equilibrium conditions at the boundary between two regions $(r = a)$

$$W^{(i)} + W^{(s)} = W^*, \quad y_r^{(i)} + y_r^{(s)} = y_r^*, \quad y_q^{(i)} + y_q^{(s)} = y_q^* \qquad (10)$$

$$M_r^{(i)} + M_r^{(s)} = M_r^*, \quad M_q^{(i)} + M_q^{(s)} = M_q^*, \quad Q_r^{(i)} + Q_r^{(s)} = Q_r^* \qquad (11)$$

where Q_r is shear forces. M_r and M_q are bending moments and the values depend on the plate bending rigidity $D = EI/(1-n^2)$. The delamination can be modeled by changing D to the bending rigidity of the inhomogeneity D^* for $r \pounds a$ and the detail of calculating D^* will be discussed in Section 2.3. Once the unknown expansion coefficients are determined, the scattered wave amplitudes of the A$_0$ Lamb wave can then be calculated using Eqs. (2) – (4).

2.2. *Born approximation*

Different to the WFE method described in Section 2.1, the Born approximation is applicable to irregularly shaped inhomogeneities, and hence, it has been commonly used in inverse scattering problems, such as diffraction tomography[19] and the eigenfunction backpropagation method[24]. Using the Born approximation to the Mindlin plate theory and assuming a far-field condition, the scattered wave solutions can be approximated as[23]

$$W^{(s)} \approx W^B(r,q) = \sqrt{\frac{2}{\rho k_1 r}} e^{i\left(k_1 r - \frac{\rho}{4}\right)} \left[-d_1 g l_1 k_1^2 D\left(\cos^2 q + n \sin^2 q\right) - d_2 \frac{1}{l_1} g k^2 Gh\left(1 - l_1\right)^2 \cos q \right.$$

$$\left. + d_3 g l_1 r I W^2 \cos q + d_4 \frac{grhW^2}{l_1 k_1^2} \right] \left[2\rho k_1 a \frac{J_1\left(k_1 a\sqrt{2 - 2\cos q}\right)}{\sqrt{2 - 2\cos q}} \right] \quad (12)$$

and $g = i/4D(k_1^2 - k_2^2)$. h is the plate thickness. d_l for $l = 1,2,3,4$ are nonzero within the region of inhomogeneity but vanish outside the region. The damaged plate properties $D^* = D\left(1 + d_1\right)$, $k^2 Gh^* = k^2 Gh\left(1 + d_2\right)$, $rI^* = rI\left(1 + d_3\right)$ and $rh^* = rh\left(1 + d_4\right)$ can be calculated by d_l to represent different types of defects.

2.3. *Modeling delamination as a cylindrical inhomogeneity*

One of the commonly used modeling techniques is to model the delamination in thin layered isotropic plates as a base plate separated into two individual sub-plates at the delaminated region, especially for modeling the delamination using a FE method[25]. This delamination model is suitable for Lamb wave problems as the delamination creates a discontinuity along the base plate at the delaminated region, in which the waveguide is divided into the upper and lower sub-waveguides with reduced bending rigidity D^* as shown in Figure 1. h_u and h_l shown in Figure 1 are thickness of the upper and lower sub-waveguides. Using the WFE method and Born approximation highlighted in Sections 2.1 and 2.2, the delamination can be modeled as an inhomogeneity with reduced bending rigidity D^*. The individual bending rigidities of the upper and lower sub-waveguides are $D^*_{upper} = Eh_u^3/12(1 - n^2)$ and $D^*_{lower} = Eh_l^3/12(1 - n^2)$, and hence, the bending rigidity of the inhomogeneity can be calculated by $D^* = D^*_{upper} + D^*_{lower}$.
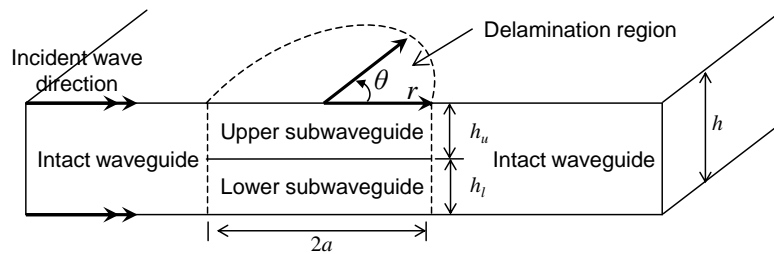

Fig. 1. Schematic diagram of the cross section at the delamination for the analytical model

2.4. *Three-dimensional explicit finite element simulation*

One of the objectives in the current study is to determine the accuracy of using an inhomogeneity to model A_0 Lamb waves scattered in response only to the geometry

change at the delaminated region. Two $180 \times 180 \times 0.8$ mm^3 aluminum plates are assumed bonded together to form a 1.6 mm thick layered isotropic plate. It has been proved that the low frequency A$_0$ Lamb wave is not sensitive to the presence of the thin adhesive layer in the bonded plate as low frequency A$_0$ Lamb wave is characterized by bending of the plate[15]. Hence, the effect of the adhesive layer on the A$_0$ Lamb wave can be safely ignored. The layered isotropic plate is modeled using a 3D explicit FE method in LS-DYNA. The Young's modulus, shear modulus, Poisson's ratio and density of the aluminum are 68.9 GPa, 26 GPa, 0.33 and 2700 kg/m^3, respectively. Eight-noded, 3D reduced-integration, solid brick elements with hourglass control and three degrees-of-freedom at each node are used to model each layer of the isotropic plate, and hence, eight layers of solid brick elements are throughout the thickness of the plate. The excitation signal is a 140 kHz narrowband six-cycle sinusoidal tone burst pulse modulated by a Hanning window. The excitation location is at $r = 90$ mm and $q = 180°$. The wavelength of 140 kHz A$_0$ Lamb wave is 8.78 mm. The in-plane dimension of the solid brick elements is around 0.4×0.4 mm^2 and the thickness is 0.2 mm, which ensures that there are at least 20 nodes per wavelength.

The circular delamination is modeled by duplicating the FE nodes along the interface of the debonding, to which the FE nodes are not connected. The delamination model splits the plate into two sub-waveguides of different displacement fields at the delaminated region.

Two simulations, one is the intact plate and the other one is the identical plate but having a delamination, are carried out in the study. The scattered A$_0$ Lamb waves are extracted by calculating the difference between the signals from the intact plate and the plate with the delamination. In this study only the out-of-plane displacement of 36 nodal points located at $r = 40$ mm, which ensures the evanescent waves can be ignored, and $0° £ q £ 360°$ with 10° step increments are calculated in the simulations. It should be noted that the calculated displacements are normalized by the out-of-plane displacements of the outgoing excitation pulse at the center of the delamination position in the intact plate. After that a scattering directivity pattern (SDP)[10,21] is calculated by determining the maximum absolute amplitude of the scattered wave in time domain. In this study, the FE simulation results are used as a benchmark and are compared with the results calculated by the WFE method and Born approximation. The same FE model was verified through comprehensive experimental studies[10].

3. A$_0$ Lamb Wave Scattering Characteristics

The SDPs calculated by the WFE method, Born approximation and FE simulations are shown in Figure 2. They are indicated as solid lines, dashed lines and crosses, respectively. Delaminations with diameters 8.55 mm, 10.39 mm and 14.05 mm located at the mid-thickness of the plate are considered in Figure 2. The bending rigidity within the delaminated region is $D^* = 0.25D$. The delamination diameter to wavelength ratios R are 0.88, 1.08 and 1.45, respectively.

Figure 2 shows that there is very good agreement between the results of the WFE method and FE simulations in the forward scattering amplitudes. This shows that the WFE method is able to predict the A_0 Lamb wave scattering at the delamination in directions $90° £ q £ 270°$. The Born approximation underestimates the amplitudes of the forward scattered waves, although it still predicts the forward scattering patterns. The discrepancy between the FE simulation and the Born approximation results is because the A_0 Lamb wave scattering at the delamination is outside the assumption of the weak inhomogeneity.
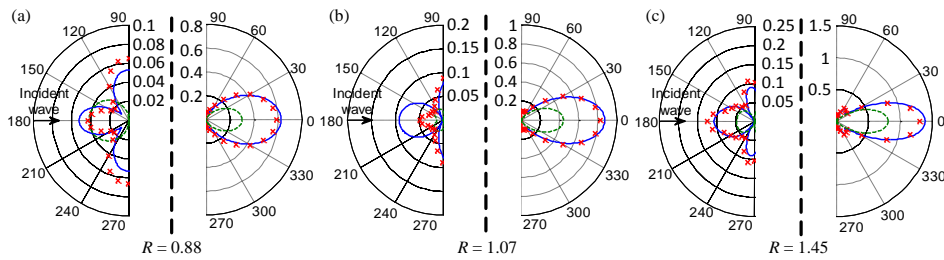

Fig. 2. Analytical (solid lines), approximated (dashed lines) and FE (crosses) results of SDP for delaminations located at mid-thickness of the layered isotropic plate

For the backward scattering amplitudes, the discrepancy between the results of the Born approximation and FE simulations is even greater than for the forward scattering amplitudes. The Born approximation underestimates the backward scattering amplitudes, but is still able to provide a reasonable prediction of the backward scattering patterns. Comparing the results of the WFE method and FE simulations, a reasonable agreement is observed in the backward scattering amplitudes and the backward scattering pattern. However, there is a larger discrepancy for the results of $R = 1.07$.

Once the SDP of the WFE method, FE simulations and Born approximation have been studied, a comprehensive analysis is considered for a range of delamination diameter, in which is carried out by changing the delamination diameter while keeping the excitation frequency at 140 kHz. Figures 3a, 3b and 3c show the forward scattering amplitudes at $q = 0°$, $20°$ and $40°$ for a range of R values. Solid lines, dashed lines and circles indicate the results of the WFE method, Born approximation and FE simulations. Good agreement is observed between the results of the WFE method and FE simulations. The results of the backward scattering amplitudes at $q = 180°$, $200°$ and $220°$ are shown in Figures. 3d, 3e and 3f, respectively. The trends of the backward scattering amplitudes at these directions behave as a sine function ramping upward. Compared to the results of the orthotropic plate, shown in Figures 8 and 9 of paper[21], the results of the WFE and FE simulations in Figure 3 show better agreement. This proves that the inhomogeneity with modeling the plate divided into two individual sub-waveguides at the delaminated region is a suitable model to predict the Lamb wave scattering at delamination in thin layered isotropic plates. In the case of composite laminates, this also implies that the stacking sequence influence on the A_0 lamb wave

have to be included in the analytical solutions for better prediction results.

For the Born approximation, which is the fundamental framework in LWDT, there is a larger discrepancy between the results of the Born approximation and FE simulations in both forward and backward scattering directions. The discrepancy becomes obvious for increasing delamination diameter to wavelength ratio. The comprehensive analysis in Figure 3 shows that the Born approximation is still able to provide a reasonable prediction in both forward and backward scattering for the delamination diameter to wavelength ratio R smaller than 0.35. The finding is useful for delamination detection with a known targeted range of delamination size as the frequency of the incident wave can be selected to ensure the value of R having a reasonable prediction in scattering by the Born approximation.
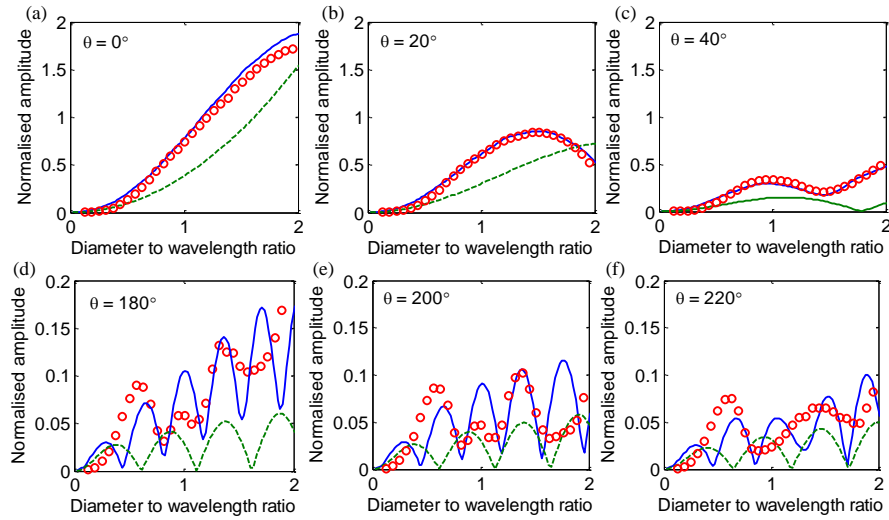

Fig. 3. Analytical (solid lines), approximated (dashed lines) and FE (circles) results of normalized forward ($q = 0°$, 20° and 40°) and backward ($q = 180°$, 200° and 220°) scattered wave amplitudes as a function of R for delaminations located at mid-thickness of the layered isotropic plate

A thin layered isotropic plate made by aluminum plates with different thicknesses are also considered in this study. The thickness of the base and top aluminum plates are 1 mm and 0.6 mm, respectively. Hence, the delamination is assumed at 3/8 total thickness below the top surface of the layered isotropic plate. The results of the delamination with $R = 0.88$, 1.07 and 1.45 are shown in Figure 4. It should be noted that the value of R is the same as those as shown in Figure 2. The only difference is that the delaminations are located at different through thickness location of the plate. It is expected that there is a mode conversion effect in the Lamb wave scattering. The reduced bending rigidity within the bonded region is $D^* = 0.3D$. Comparing the FE simulation results in Figures 2 and 5, the forward scattering amplitudes have different magnitudes but still have similar forward scattering patterns. However, Figure 5 shows that the backward scattering amplitudes and

patterns are quite different to those in Figure 2.

Overall, there is still reasonable agreement between the results of the WFE method and FE simulations, especially for the forward scattering patterns. The backward scattering amplitudes and patterns are not well predicted by the WFE method or the Born approximation. The discrepancy in the forward and backward scattering is mainly due to the mode conversion effect and is not considered in the WFE method or the Born approximation. This shows that the mode conversion effect needs to be accounted for in the WFE method and the Born approximation to further improve the accuracy of the scattering prediction.
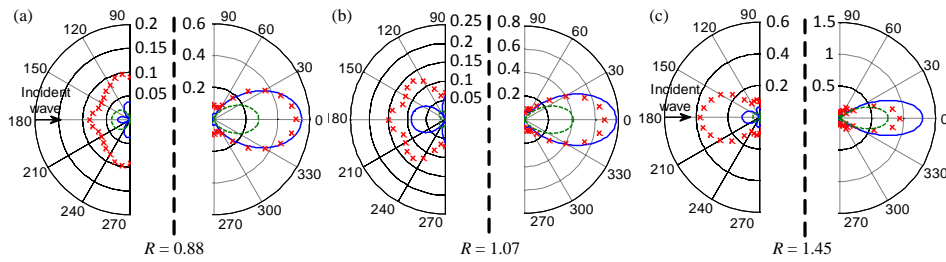

Fig. 4. Analytical (solid lines), approximated (dashed lines) and FE (crosses) results of SDP for delaminations located at 3/8 total thickness below the top surface of the layered isotropic plate

4. Conclusions

An investigation on the accuracy of modeling the delamination as an inhomogeneity to predict the A_0 Lamb wave scattering characteristics has been studied by comparing the results of the WFE method, Born approximation and 3D explicit FE simulations. The study has validated the fundamental assumption that the delamination can be modeled as a waveguide divided into two sub-waveguides for the A_0 Lamb wave problems.

An experimentally verified 3D FE model has been used as a benchmark to assess the accuracy of the WFE method and Born approximation. The results have showed that the WFE method with reduced bending rigidity at inhomogeneity can well predict the scattering amplitudes of A_0 Lamb waves at delaminations in thin layered isotropic plates, especially in the forward directions. For the backward scattering, although the inhomogeneity is not able to accurately predict the amplitudes, it still provides a well prediction of the backward scattering patterns, especially for the trend of the amplitudes when the diameter of the delaminated region increases. For Born approximation, the results are not as good as the results of the WFE method. However, the Born approximation is still able to provide a reasonable prediction for both forward and backward scattering for delamination diameter to wavelength ratio R smaller than 0.35. For a known targeted range of delamination size, this finding is useful for characterizing delamination in thin layered isotropic plates by LWDT, in which the Born approximation is the fundamental framework.

Overall, the results have showed that the inhomogeneity is able to predict the A_0 Lamb wave scattering at delaminations and it is possible to employ it in damage

characterization. The study has showed that the mode conversion effect needs to be accounted for in the WFE method and Born approximation if the region of delamination is not located at mid-thickness of the plate and this is the next steps of this research.

The results of the study have also suggested that an improvement of the analytical solution to accurately predict the Lamb wave scattering at delamination in composite laminates can be achieved if stacking sequence influence is included in the analytical solutions. There is a potential to extend the LWDT for characterizing delaminations in composite laminates.

Acknowledgments

References

1. Rose, J.R., A baseline and vision of ultrasonic guided wave inspection potential. *J. Pressure Vessel Technol.* **124** (2002) 273–282.
2. Veidt, M., Ng, C.T., Hames, S. and Wattinger, T., Imaging laminar damage in plates using Lamb wave beamforming. *Adv. Mater. Res.* **47–50** (2008) 666–669.
3. Ng, C.T., Veidt, M. and Lam H.F., Guided wave damage characterisation in beams utilising probabilistic optimization. *Eng. Struct.* **31** (2009) 2842–2850.
4. Ng, C.T., Bayesian model updating approach for experimental identification of damage in beams using guided waves. *Struct. Health Monitor.* **13** (2014) 359–373.
5. Vemula, C. and Norris, A.N., Flexural wave propagation and scattering on thin plates using Mindlin theory. *Wave Motion* **26** (1997) 1–12.
6. Grahn, T., Lamb wave scattering from a circular partly through-thickness hole in a plate. *Wave Motion* **37** (2003) 63–80.
7. Cegla, F.B., Rohde, A. and Veidt, M., Analytical prediction and experimental measurement for mode conversion and scattering of plate waves at non-symmetric circular blind holes in isotropic plates. *Wave Motion* **45** (2008) 162–177.
8. Moreau, L., Caleap, M., Velichko, A. and Wilcox, P.D., Scattering of guided waves by through-thickness cavities with irregular shapes. *Wave Motion* **48** (2011) 586–602.
9. Moreau, L., Caleap, M., Velichko, A. and Wilcox, P.D., Scattering of guided waves by flat-bottomed cavities with irregular shapes. *Wave Motion* **49** (2012) 375–387.
10. Ng, C.T. and Veidt, M., Scattering of fundamental anti-symmetric Lamb wave at delaminations in composite laminates. *J. Acoust. Soc. Am* **129** (2011) 1288–1296.
11. Ng, C.T. and Veidt, M., Scattering characteristics of Lamb waves from debondings at structural features in composite laminates. *J. Acoust. Soc. Am* **115** (2012) 115–123.
12. Ng, C.T., On the selection of advanced signal processing techniques for guided wave damage identification using a statistical approach. *Eng. Struct.* **67** (2014) 50–60.
13. Cuc, A. and Giurgiutiu, V., Disbond detection in adhesively-bonded structures using piezoelectric wafer active sensors. in *Proc. SPIE* **5394** (2004) 66–77.
14. Shelke, A., Kundu, T., Amjad, U., Hahn, K. and Grill, W., Mode-selective excitation and detection of ultrasonic guided waves for delamination detection in laminated aluminum plates. *IEEE Trans. Ultrason. Ferroelectr. Freq. Control* **58** (2011) 567–577.
15. Lowe, M.J.S. and Cawley, P. The applicability of plate wave techniques for the inspection of adhesive and diffusion bonded joints. *J. Nondestr. Eval.* **13** (1994) 185–200.

16. Ng, C.T. and Veidt, M. A Lamb-wave-based technique for damage detection in composite laminates. *Smart Mater. Struct.* **18** (2009) (074006)1–12.
17. Giurgiutiu, V. Piezoelectric wafer active sensors for structural health monitoring of composite structures using tuned guided waves. *AIAA J.* **48** (2011) 565–581.
18. Ng, C.T., Veidt, M. and Rajic, N. Integrated piezoceramic transducers for imaging damage in composite laminates. in *Proc. SPIE* **7493** (2009) (74932M), 1–8.
19. Rose, L.R.F. and Wang, C.H., Mindlin plate theory for damage detection: Imaging of flexural inhomogeneities. *J. Acoust. Soc. Am*. **127** (2010) 754–763.
20. Chan, E., Wang, C.H. and Rose, F.L.R. Characterization of laminar damage in an aluminum panel by diffraction tomography based imaging method using Lamb waves. in *Proc. 7th European Workshop on Structural Health Monitoring*, Nantes, France, 73-79, (July 2014).
21. Veidt, M. and Ng, C.T. Influence of stacking sequence on scattering characteristics of the fundamental anti-symmetric Lamb wave at through holes in composite laminates. *J. Acoust. Soc. Am.* **129** (2011) 1280–1287.
22. Ng, C.T., Veidt, M., Rose, L.R.F. and Wang, C.H., Analytical and finite element prediction of Lamb wave scattering at delaminations in quasi-isotropic composite laminates. *J. Sound Vib*. **331** (2012) 4870–4883.
23. Wang, C.H. and Chang, F.K. Scattering of plate waves by a cylindrical inhomogeneity. *J. Sound Vib*. **282** (2005) 429–451.
24. Lin, F., Nachman, A.I. and Wang, R.C. Quantitative imaging using a time-domain eigenfucntion method. *J. Acoust. Soc. Am*. **108** (2000) 899–912.
25. Kudela, P. and Ostachowicz, W. A multilayer delaminated composite beam and plate elements: reflections of Lamb waves at delamination. *Mech. Adv. Mater. Struct*. **16** (2009) 174–187.